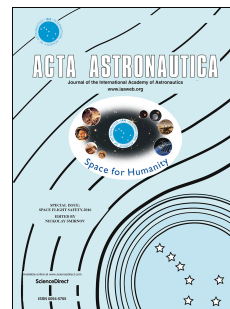# Accepted Manuscript

Ignition and combustion of air/fuel mixture in a long tube induced by microwave subcritical streamer discharge

M.P. Bulat, P.V. Bulat, P.V. Denissenko, I.I. Esakov, L.P. Grachev, K.N. Volkov, I.A. Volobuev

Please cite this article as: M.P. Bulat, P.V. Bulat, P.V. Denissenko, I.I. Esakov, L.P. Grachev, K.N. Volkov, I.A. Volobuev, Ignition and combustion of air/fuel mixture in a long tube induced by microwave subcritical streamer discharge, *Acta Astronautica* (2019), doi: https://doi.org/10.1016/j.actaastro.2019.01.028.

Ignition and combustion of air/fuel mixture in a long tube induced by microwave subcritical streamer discharge

M.P. Bulat[1], P.V. Bulat[1, 2, *], P.V. Denissenko[3], I.I. Esakov[4], L.P. Grachev[4], K.N. Volkov[5], I.A. Volobuev[2]

[1]Baltic State Technical University, 190005, St Petersburg, Russia

[2]ITMO University, 197101, St Petersburg, Russia

[3]University of Warwick, CV4 7AL, Coventry, United Kingdom

[4]Moscow Radiotechnical Institute of Russian Academy of Sciences, 117519, Moscow, Russia

[5]Kingston University, SW15 3DW, London, United Kingdom

Abstract

There have been consistent efforts in developing more efficient combustion for propulsion systems. Ignition and combustion control using cold and non-thermal plasma in microwave discharges have become a major topic of interest. In this study, a microwave subcritical streamer discharge is used to initiate ignition and combustion of premixed air/fuel mixture in a long cylindrical tube. The streamer discharge is arising on the internal surface of the dielectric tube using a passive vibrator in a single pulse regime at atmospheric pressure and temperature. The propagation speed of the combustion front in the quartz cylindrical tube filled by the air/propane mixture is analyzed experimentally and numerically. The streamer discharge creating a multitude of ignition points provides practically instantaneous ignition of the mixture in the entire volume. The speed of streamer induced combustion front has been shown to be higher compared to that initiated by a spark. Increasing the length of streamer discharge leads to increasing the flame propagation speed. The combustion efficiency has also been shown to be higher when using the microwave streamer ignition.

Keywords

Flight safety; Microwave-assisted combustion; Streamer discharge; Air/fuel mixture; Ignition; Combustion

1 Introduction

Flight safety and sustainability of the propulsion systems in aerospace engineering are strongly linked to the ignition technology and combustion control. The propulsive performance of air-breathing pulse detonation engiones (PDEs) has been theoretically and numerically studied over a wide range of system configurations, operating parameters and flight conditions [1, 2], and various ignition systems (e.g., electric discharge, microwave discharge, laser radiation, laser-induced breakdown) have been tested to achieve simultaneous space ignition via multiple ignition points throughout the combustion chamber [3–8].

Plasma-assisted combustion is able to provide additional combustion control, which is necessary for ultra-lean flames, high-speed flows, cold low-pressure conditions, detonation initiation [9,10]. The idea of using plasma methods of fuel ignition is based on non-equilibrium generation of chemically active particles, accelerating the combustion process [11]. The possibilities of a non-equilibrium electric discharge are experimentally demonstrated in [12]. The results of experimental and numerical analysis of plasma-assisted combustion at a normal and high pressures and temperatures are presented in [13]. The spatial and temporal dynamics of a pulsed microwave plasma is studied in [14]. The experimental results highlight the effects of the pulse repetition frequency on the discharge dynamics. Electrical breakdown resulting in the ignition of a low-pressure low-current glow discharge in long (length much larger than the diameter) tubes is studied in [15].

Microwave plasma has shown potential improved ignition characteristics [16]. Microwave plasma can be generated at pressures from 10^{-5} torr up to atmospheric pressure using pulse and continuum regimes. However, ignition of air/fuel mixture with a microwave beam requires a powerful microwave generator. For example, at air pressure 760 torr the breakdown takes place at the power larger than 10^6 W/cm.

Among the various types of discharges studied, the microwave streamer discharge has demonstrated promising characteristics for ignition at low initial pressures and temperatures [17]. One of the main properties of a developed streamer discharge is that it absorbs almost all the electromagnetic energy incident on it. Another important feature of a streamer discharge is that the streamer grows into a region of the electromagnetic beam where the amplitude of the electric component of the initial field is substantially lower than the critical one.

A streamer discharge in air at atmospheric pressure is a thin plasma filament (typical radius of the order of 20–100 μm) with a bright streamer head. The streamer velocity is of the order of 10^7–10^8 cm/s, that is one hundredth of the speed of light in the vacuum [18]. The ignition is initiated over the whole volume where the plasma filaments propagate. The temperature of fuel mixture at the point of ignition is not higher than 400 K. The peak of electric field in the streamer head reaches 4–7 times the breakdown field [19].

The presence of seed electrons in front of the propagating streamer head plays a critical role in the propagation of streamer. For some conditions, these seed electrons are present in the gas, and gas can be efficiently pre-ionized by the previous discharge [20]. When the pre-ionization of the gas is too low, the photo-ionization mechanism supports the streamer propagation [21]. The appearance of filamentary plasma channel is associated with development of ionization-overheating instability process in the plasma of microwave discharge, which is accompanied by a powerful ultraviolet radiation from the discharge zone [23]. Numerical simulations of the streamer discharge, including the transition from avalanche to streamer and streamer propagation, are carried out in [24].

In this study, possibilities of the use of microwave radiation to initiate combustion of premixed air/fuel mixtures in the quartz cylindrical tube are investigated experimentally and numerically. The streamer discharge is induced by the electrical field strength which is smaller than the critical one. Electromagnetic beam has sizes about tens of wavelength of microwave radiation along its propagation and about some units of a wavelength in the radial direction.

2   Forms of microwave discharges

When a high-power electromagnetic beam with intensity E_0 is focused at a point and interacts with a gas, the gas breaks down and becomes highly ionized. This process is accompanied by a light flash and generation of sound. There is a threshold intensity of the electromagnetic beam, E_c, at which gas breakdown is observed. The discharge is overcritical if $E_0 > E_c$, and the discharge is subcritical if $E_0 < E_c$ (special facilities are used to induce a discharge). Microwave beam is similar to optical beam because it is bounded by the surface transition through which leads to a sharp changes in energy distribution. However, transversal dimension of the microwave beam is small compared to optical beam making it about several wavelengths, λ (in optics, transversal dimension of the beam is about $10^5\lambda$).

High- and medium-pressure discharges induced by quasi-optical microwave beams in air are classified in [25] based on experimental observations. Diffuse, streamer, overcritical, subcritical and deep subcritical streamer discharges are distinguished. The domains of existence of each form of discharge are determined as functions of air pressure and electrical field strength (wavelength is fixed). The distinct observed forms of microwave discharges are represented in the Figure 1, where E_0 is the electric field of the microwave beam in the discharge region and E_c is the critical breakdown of the electric field. They are designated by Roman numerals I–V, respectively. These domains are determined by analyzing a series of time-integrated frames of discharges (the exposition time exceeds the time of pulse) operating at different initial field strengths and air pressures [25].

Lines 1, 2 and 3 divide diagram into a number of sub-regions. Line 1 represents the pressure dependence of the critical field (this is Paschen-like line in microwave range). It is possible to ignite a self-sustained discharge without any initiated settings above this line, while below it a discharge has to be initiated with some additional settings such as a special designed metal vibrator or a preliminary discharge introduced by laser. There is a narrow transition region below line 1 ($E_0 < E_c$), where a weak reflection of microwave radiation from an initiated subcritical discharge leads to self-sustained air breakdown in the microwave beam in front of discharge. Line 2 is a pressure boundary (about several tens torr) that separates diffuse discharges at low pressure from streamer discharges at high pressure. There is an air pressure range (the hatched region), in which it is difficult to distinguish diffuse and streamer discharges. Line 3 separates the subcritical and deep subcritical discharges. The difference between the subcritical and deep subcritical discharges is that the streamers remain attached to the initiator for deep subcritical discharge. The diffuse discharge plasma in the subcritical region also remains attached to the initiator. In this study, a deep subcritical discharge at normal atmospheric pressure ($p = 760$ torr) is used.

3   Diagnostic method

Experimental setup and technique have been developed at the Moscow Radiotechnical Institute (MRTI) of Russian Academy of Sciences (RAS). These were adopted for the current study dealing with microwave-induced combustion in the quartz cylindrical tube.

3.1   Experimental setup

The test rig shown in the Figure 2 consists of a microwave power source, a vacuum chamber, a set of devices providing the microwave radiation transport from the source to the chamber, focusing elements and a set of diagnostic equipment. A main component of the microwave power source is a pulsed magnetron generator. Its power supply is provided by a modulator
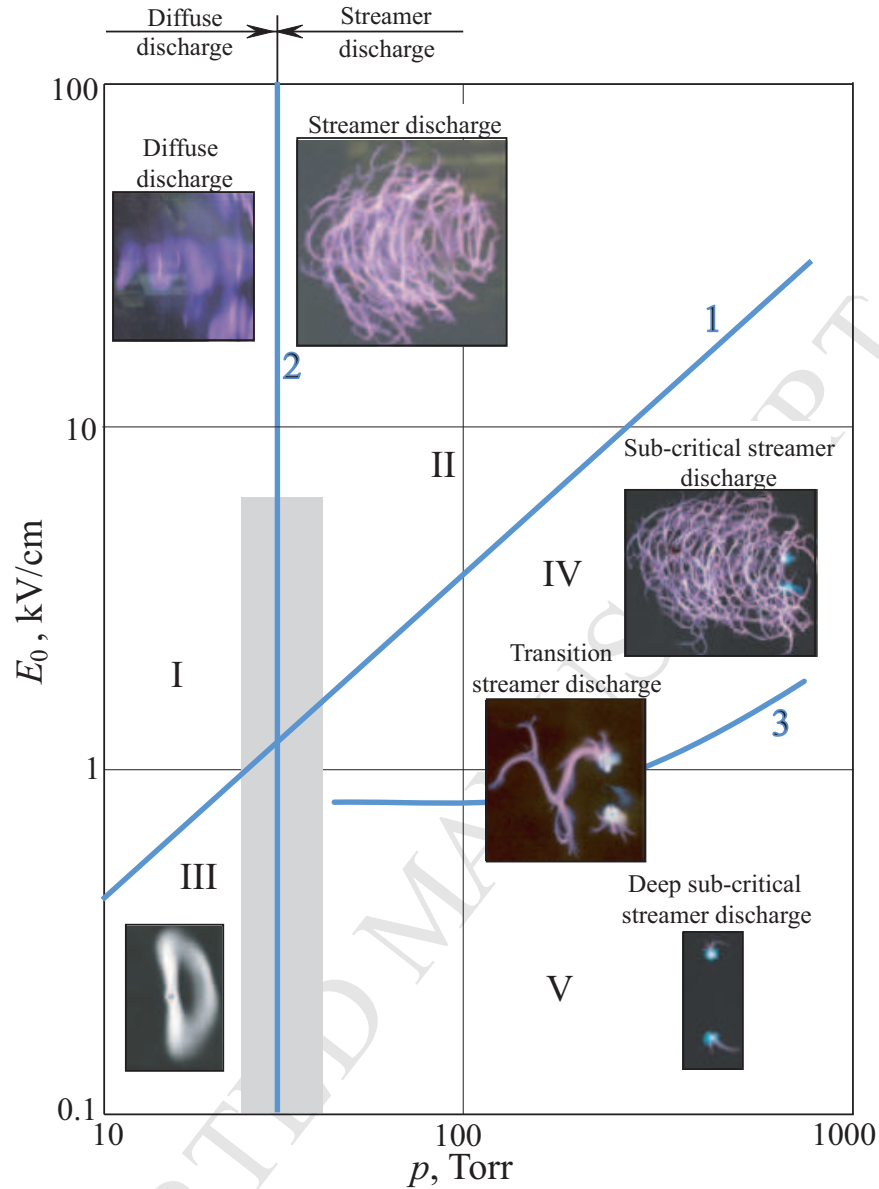
Figure 1. Different forms of microwave discharges in air for $\lambda = 8.9$ cm [25]

based on a partial discharge of a storage capacitor. The maximal pulsed power of the magnetron is about 10^7 W. The microwave wavelength is 8.9 cm. The modulator generates rectangular microwave pulses and provides discrete adjustment of their duration from 4 to 40 μs with 4 μs step. The maximal repetition frequency of the pulses is 1 Hz. In this study, single pulses are used. Magnetron output is a rectangular 72×34 mm^2 waveguide.

The vacuum chamber consists of two parts. The first part is a stationary metal cylinder with 630 mm diameter polystyrene lens, through which the microwave radiation enters the chamber. On the periphery there are located vacuum microwave and high voltage sockets, through which the information input and output is made. At the internal part of the cylinder, four aluminum cores (1600 mm length and 40 mm diameter) are screwed normally to it and in regular intervals on 680 mm diameter. Various equipment (focusing mirror, microwave absorbers) is fixed on them. The second part of the chamber is a stainless steel cylinder (1700 mm length and 800 mm diameter) which is coaxial with the first part, and can be bolted to it. The second part is fixed to a wheel carriage. It can be rolled away to open the internal volume of the chamber to provide a convenient access.
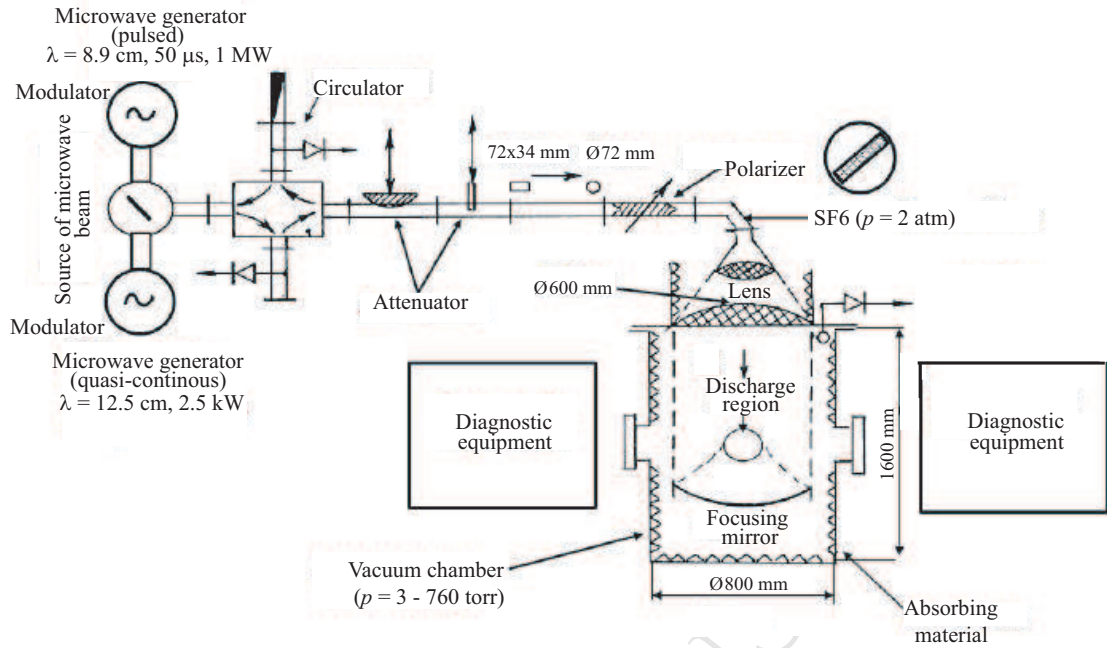
Figure 2. Experimental setup consisting of source of microwave beam, modulator, circulator, attenuator, polarizer, lens system, vacuum chamber, diagnostic equipment, discharge region, focusing mirror

The vacuum chamber has four windows. Three of them have 200 mm diameter and one (looking down) has 400 mm diameter. On the windows there can be fixed 20 mm thick optical glass plates, organic glass water filled illuminators (for visual supervision and diagnostics of processes in the chamber) or metal plates with equipment. A microwave absorptive material coating of the internal surfaces of the vacuum chamber makes it free from microwave echo (20 dB level). Rubber gasket seals make the chamber water-proof.

The installation is equipped with a forevacuum pump providing pressure range from 3 to 760 torr. Pressure measurements are carried out by a pressure sensor with accuracy ± 1.5 torr. The chamber is tested down to minimum pressure of 10^{-5} torr.

The microwave radiation from magnetron is transported through the waveguide, which includes a circulator, an attenuator, a polarizer and a lens system. The waveguide has a rectangular cross section 72 mm^2 before the polarizer with a transition to a round cross section (76 mm diameter) at the polarizer.

A ferrite polarization type circulator plays a role of a gate. It prevents the reflected wave to cause a failure of generation of the magnetron if a disturbance of the running wave mode regime takes place in the waveguide. To control the levels of direct and reflected waves, branching-off is used. The waveguide is equipped with two adjustable attenuators. The first attenuator is based on absorption of chamber radiation by water providing 5 times reduction of the electromagnetic wave amplitude. In the second attenuator, a controlled attenuation (up to 20 times of the field amplitude reduction) results from blocking the waveguide cross section by a reflecting knife. The polarizer makes it possible to change the field polarization from linear (vertical) to circular. It contains a polystyrene 360 mm long and 12 mm thick plate, which is turned around of the waveguide axis without disassembling it. The polarization is checked by electric field sensors situated at the output end of the waveguide. A conic diffuser with a polyethylene microwave transparent diverging lens with diameter of 25 mm is attached to the waveguide. The axis of lens coincides with the axis of the lens on the first part of the chamber. The waveguide system is sealed tight and filled by

the hexafluorated sulfur (SF_6) at an overpressure of 1 atm.

The lens system consists of the lens on the target diffuser of the waveguide and the lens on the second part of the chamber. It provides input of the microwave radiation into the chamber as TEM mode wave with a flat phase front. The beam in the chamber is axisymmetric with Gaussian distribution of intensity. A metal mirror 600 mm diameter is installed in the chamber on a distance of 1 m from the lens. The mirror focuses the microwave radiation on an axis of the chamber illuminators.

The installation is equipped with a set of diagnostic devices for measuring microwave field amplitude and polarization, time integrated and high-speed camera photo registration of plasma radiation at the discharge processes, spatial mean values of the plasma electron concentration, registration of gas dynamic perturbations using shadow method, parameters of shock waves from the discharge area, spatial mean gas temperature of the discharge region.

Air/propane mixture is selected for the experiments because propane combustion is one of the most classical and the most studied processes.

3.2 Experimental procedure

Some details of the experimental setup related to initiation of a microwave discharge are shown in the Figure 3. The test rig includes a microwave generator that produces electromagnetic waves with a frequency 3.4 GHz corresponding to the wavelength 8.9 cm (Figure 3a). Duration of the microwave pulse is 40 μs, and the power of the beam varies from 10^2 to 10^6 W. Electromagnetic wave passes polystyrene lens and falls onto the axisymmetric metal concave spherical mirror with 450 mm curvature radius, 685 mm diameter and 158 mm depth (Figure 3b). Electromagnetic wave reflected from the mirror is focused on the centreline on 225 mm distance from the center of spherical mirror surface or 67 mm distance from the mirror mouth.
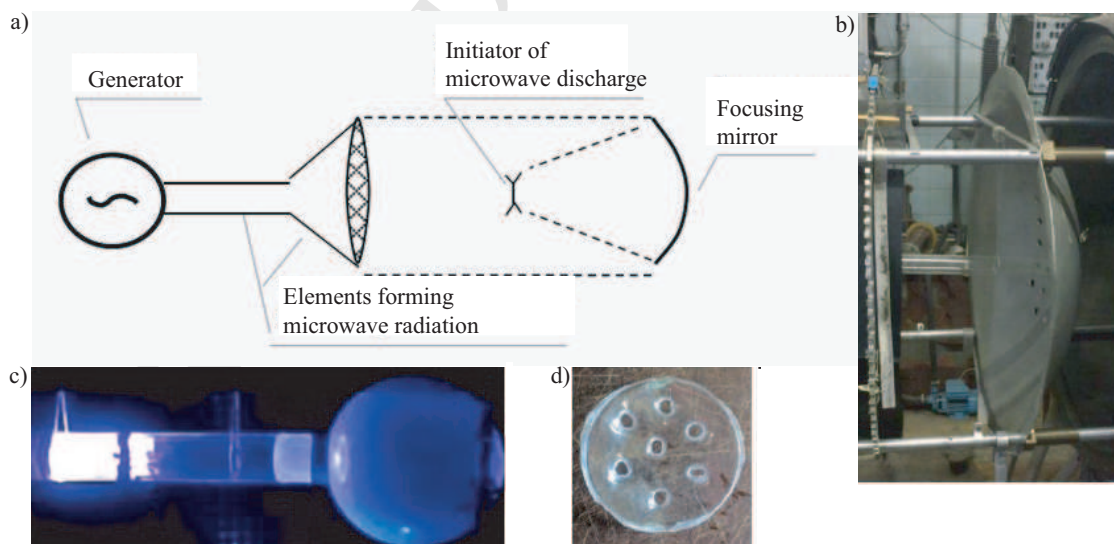

Figure 3. Details of the experimental test rig

The quartz tube is placed in the focus region of the quasi-optical beam. One end of the tube is closed, and another one is open. The tube length is 500 mm, and its internal diameter is 30 mm. A rubber balloon is attached to the open end of the tube (Figure 3c) separating air/fuel mixture from the surrounding. A polystyrene protective membrane is attached to the open end of the tube (Figure 3d) preventing balloon damage at air pumpage from the tube. A small tube is connected to the membrane which is used to pumped out

the air and to supply air/propane mixture. Fuel and oxidizer concentrations are controlled by varying partial pressures. The measurements are performed with stoichiometric mixture. The discharge initiator is placed on 27 mm distance from the closed end of the tube.

Development of the streamer and the propagation of the flame front has been recorded using a monochrome high-speed camera Phantom v.2511 with the frame rate of up to 750,000 frames/s and the color Nikon1 J2 camera at a frame rate of 1200 frames/s. The speed of the flame front propagation and the induction time from the moment of the discharge to the beginning of combustion reaction have been measured.

To study the effect of microwave field intensity on the type of generated discharge and the nature of combustion, the initiator is placed in the focus of the mirror and then shifted along the axis. The results of measurements of the electric field strength are shown in the Figure 4a. In the tests, power and energy of microwave beam remain the same. To vary energy of the microwave discharge, the discharge initiator shifts relative to the focus, and the electric field strength and energy release are found from the graph. The length of the streamer discharge strongly depends on the strength of electric field (Figure 4b).
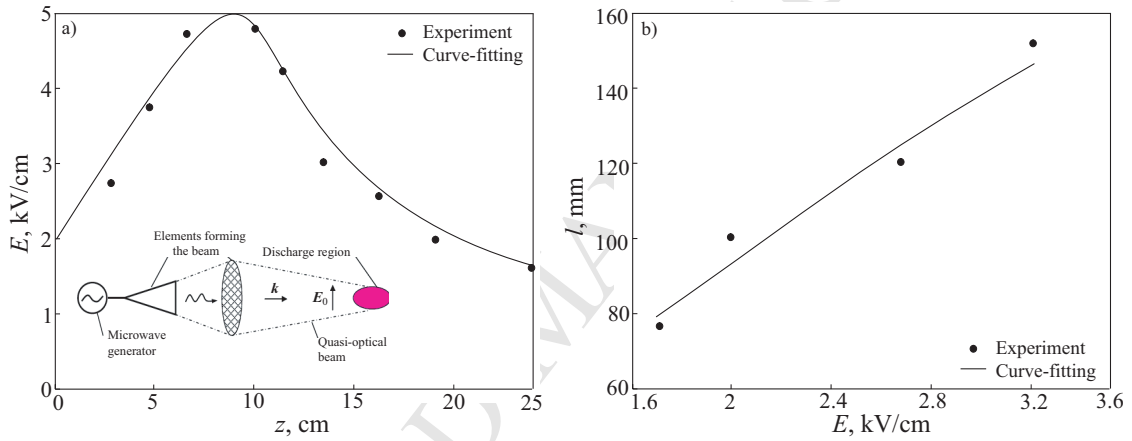

Figure 4. Electric field strength as a function of distance from the mirror edge (a) and length of the streamer discharge as a function of electric field strength (b)

The x axis is parallel to the magnetic component, and y axis is parallel to the electric component of electromagnetic field. The z axis is parallel to the direction of the beam propagation. Near the focus the electric field distribution is approximated by the Gaussian law with characteristic sizes $x_0 = 2.5$ cm and $y_0 = 5.2$ cm. Maximal electric field in the focus equals to $E_0 = 7 \times 10^3$ V/cm.

A measured normalized radial distribution of the microwave power is shown in the Figure 5 on a distance $z = 50$ cm from the lens. In the area close to the axis the dependence of power, P, on the radial coordinate, r, is approximated as

$$P = P_m \exp(-r^2/r_0^2),$$

where r is the radial coordinate and r_0 is the radius of focal spot ($r_0 = 14$ cm). The magnetron works in a regime with a maximal field $E_m = 1.3 \times 10^3$ V/cm (as measured on the axis at linear polarization and a completely opened attenuator), and the maximal power is $P_m = 2 \cdot 10^3$ W/cm^2 giving the total maximal microwave energy input as 1.2×10^6 W. Along the chamber axis the microwave beam is approximately homogeneous (on a level of 0.8).

The electrical field strength is related to the power of the beam as
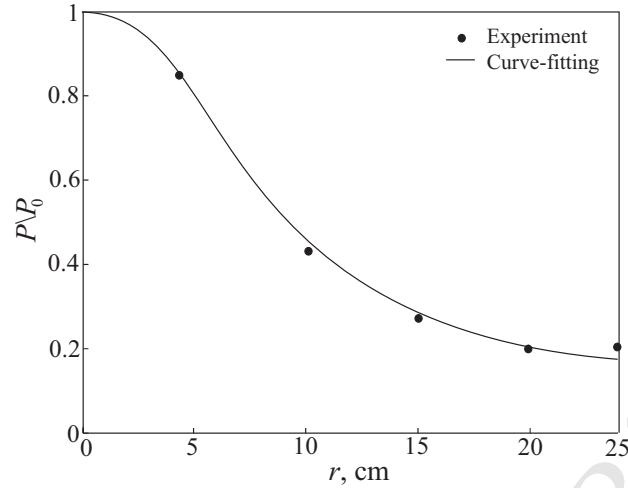
$$P = \frac{E_0^2}{2Z_0}S,$$

Figure 5. Radial distribution of normalized field intensity in the microwave beam

where $Z_0 = \mu_0 c$ is the characteristic resistance of a free space ($Z_0 = 120\pi$ Ohm, μ_0 is the magnetic constant, c is the speed of light. The cross section of the beam is ellipse, and the characteristic area of the beam is $S = 0.5\pi y_0 z_0$. The power of the beam is $P = 620$ kV assuming that $E_0 = 4.8$ kV/cm. The duration of the pulse is 40 μs, and energy of the beam is $Q = 24$ J. The power and energy remain constant in the experiments, and discharge initiator is shifted with respect to the focus. Then, electrical field strength is found from the Figure 4, and energy of the beam is calculated.

The streamer discharge is induced on the ends of the initiator representing the metallic net with squared cells and covering internal cylindrical surface of the quartz tube (Figure 6a) and propagates towards the beam (Figure 6b). Blue points on the ends of initiator are visible in the Figure 6a, and the streamer discharge (purple color) propagates from these points.
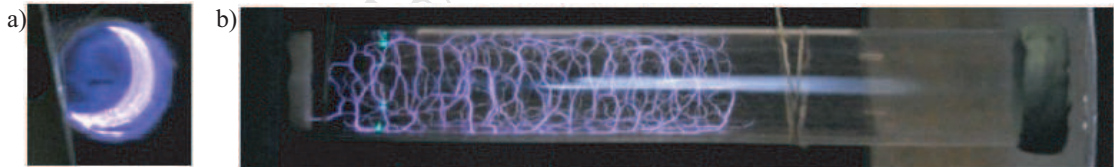

Figure 6. Streamer discharge initiated on the internal surface of the quartz tube: face view (a) and side view (b)

To develop pre-combustion chamber ignition technique, experiments and calculations of air/propane mixture ignition with the streamer discharge initiated on the internal surface of the tube were carried out. Figure 7 shows photographs of the discharge in the quartz tube at different levels of electrical field strength, E_0. The bright line is a flash from the illuminating lamp, and green points in the lower and upper parts of the tube are discharges from the ends of the initiator. The mirror is from the left, the microwave beam propagates along horizontal axis, and the vector of electric field is vertical. The tube is placed on the centreline of microwave beam. Then, it is shifted from the focus of the mirror to the right, and the length of the discharge decreases. The discharge on the internal surface of the tube is developed at large levels of electrical field. The discharge moves towards the microwave beam with the speed of kilometers per second. If E_0 is smaller than 2 kV/cm, the discharge becomes deep subcritical. It is visible on the initiator only during the microwave pulse.
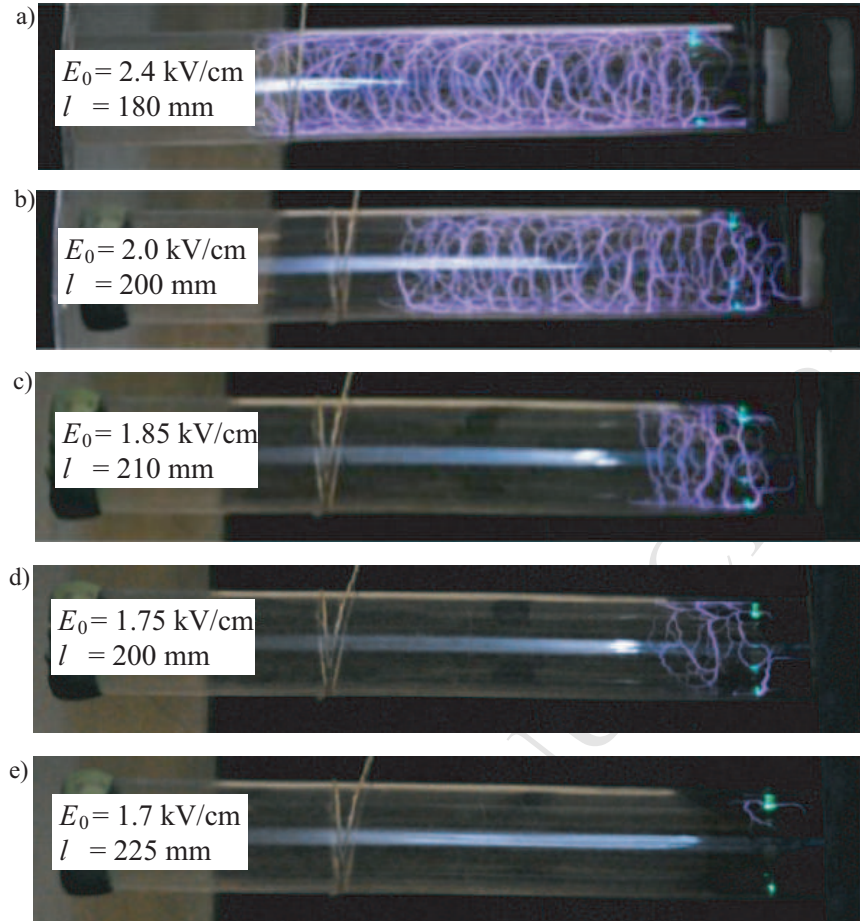
Figure 7. Development of streamer discharge for different strengths of the electric field $E_0 = 2.4$ kV/cm (a), 2 kV/cm (b) and 1.85 kV/cm

4 Numerical analysis

A streamer discharge in air at atmospheric pressure is a thin plasma filament with a bright streamer head which propagates rapidly (streamer velocity is of the order of 10^7–10^8 cm/s). Time development of streamers is much shorter than time of microwave pulse and typical time of the process. In the model, process development of plasma filaments is treated as instantaneous (from the mathematical point of view, it is based on delta-function). To simulate the energy deposition in perfect ideal gas, a step energy distribution in a finite volume depending on the size of metallic net covering internal surface of the tube is taken for an initial condition. In calculations for a perfect ideal gas, a simplified model of energy deposition is used. It ignores ionization, dissociation and chemical reactions going in a real gas at high temperatures.

Plasma is treated as an ideal gas. Geometrical model is shown in the Figure 8. A closed circular tube is filled with a premixed air/propane mixture. The length of the tube is $L = 500$ mm, and its radius is $R = 15$ mm. The width of energy release zone is $s = 1$ mm. The distance between two zones of energy release is $h = 8$ mm, and the width of the thread is 3 mm. Numerical calculations are performed for different lengths of surface streamer discharge ($l = 8, 16, 32, 64, 128$ and 144 mm). During the microwave discharge, the convective motion of the plasma is small compared to the characteristic size of the problem (radius of tube). In the numerical simulations it is assumed that energy is released instantaneously. The distance between each filament is one-tenth of the wavelength of the incident microwave.

This distance corresponds to that used in [27] to reproduce propagation of electromagnetic wave, ionization process of plasma, and shock wave formation in atmospheric microwave discharge.
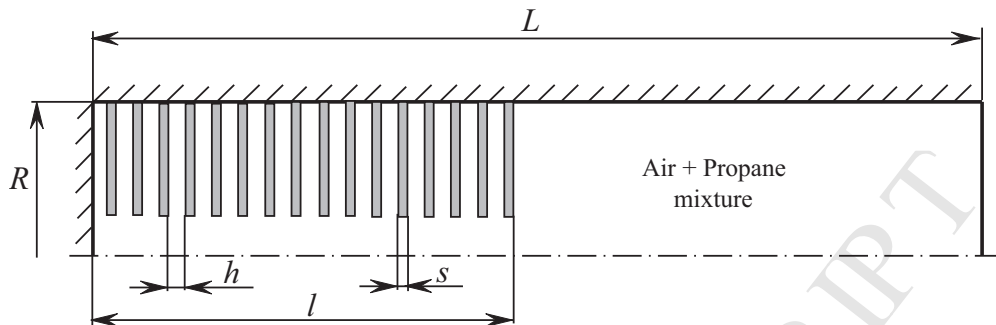

Figure 8. Cylindrical tube filled by premixed air/propane mixture

Simulation of flame propagation through a cylindrical tube involves solution of gas dynamics equations written in the axisymmetric form. Since the characteristic times of the process are rather small, there is no need to take into account viscosity and heat transfer. Therefore, the model includes conservative equations of mass, momentum, energy and species for a mixture of ideal multi-component non-viscous and non-conducting components (Euler equations). The chemical reaction is assumed to be an irreversible single step reaction between oxygen and propane, and the chemical species are C_3H_8, O_2, N_2, CO_2 and H_2O. The reaction rate of a single-step reaction is estimated using an Arrhenius-type of formulation.

The computational mesh consisting of about 1 million of cells is generated. A mesh sensitivity analysis is performed using a mesh with various number of cells. At the initial time moment, the channel is uniformly filled with stoichiometric air/propane mixture. The initial state of the mixture is set to 101,325 Pa and 300 K. The concentration of each chemical species is set so that the equivalence ratio between oxygen and propane could be 1. No-penetration boundary conditions for velocity and zero flux for scalars such as temperature and mass fraction are used at the walls. Axisymmetric boundary conditions are specified for the physical quantities on the centreline. Neumann outflow boundary conditions are applied to the outlet boundary.

The governing equations are solved numerically with the finite volume method [28] using the principle of separation of physical processes (splitting scheme). At each time sub-step, the effects of convective transfer and pressure work are first treated, then the effects of chemical transformations are taken into account. At the first step, the source term is zero, and Godunov-type method is used. The explicit Runge–Kutta scheme of the third order is used for time discretization, and MUSCL scheme is exploited for space discretization. At the second sub-step, the system of differential equations describing the gas composition change and the energy release by the chemical transformations is solved.

5   Results and discussion

The subcritical streamer discharge is formed by electric field with the intensity smaller than the minimum pulse intensity leading to the air breakdown. Streamer discharge ignition of air/propane mixture with excess oxidant ratio greater than flammability limit under normal conditions is studied. Analysis of the video tapes reveals the great variety of shapes in the discharge phenomena observed in the experiments.

The critical strength of the electric field is found from the semi-empirical equation [18]

$$E_c = 42p_{\text{torr}} \left[1 + \left(\frac{\omega}{\nu_c} \right)^2 \right]^{1/2} \quad [\text{W/cm}],$$

where ν_c is the frequency of collisions of electrons with molecules ($\nu_c = 4 \times 10^9 p_{\text{torr}}$ for air), ω is the cyclic frequency of the electric field, p_{torr} is the pressure. A linear dependence of energy threshold on air pressure takes place at high pressures. For continuous microwave radiation this dependance is shown in the Figure 9a. For a pulsed microwave radiation, a probability of air breakdown depends on the presence of free electrons in the focus region during the pulse. Figure 9b shows experimental values of critical strength of electric field for a single pulse (symbols ∘) and train of pulses with 1 Hz frequency (symbols •). Placement of the source of electrons in the focus region of microwave beam leads to decrease of threshold of air breakdown (symbols □).
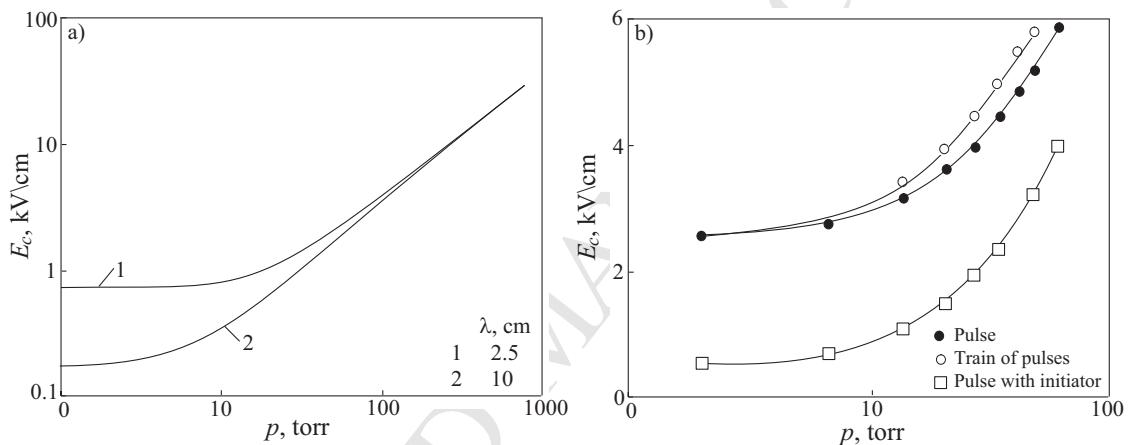

Figure 9. Dependance of threshold of air breakdown on pressure for continuous (a) and pulsed (b) radiation

Placing a conducting element in the region of microwave beam, for example, metallic sphere with radius a dimensions of which are compared to the wavelength, the electric field increases and breakdown energy decreases (Figure 10). The solid lies correspond to the calculations based on semi-empirical correlation, and symbols • and ∘ correspond to the experimental measurements.

Combustion starts along entire length of each filament. Volumetric ignition takes place not in the whole volume, in which streamer propagates. Ignition zone occupies about one third of the streamer discharge from the end of the tube (Figure 11). Discharge glow is the brightest in this region. At the strength of electric field $E_0 = 2.0$ kV/cm the flame front has a propagation speed of 15 m/s in the region occupied by of streamer discharge. Then, the flame shape becomes flatter, and its speed is lowered to about 2.5–5 m/s. The speed of combustion front lowers in 3 times if the strength of electric field drops to 1.8 kV/cm. The process is accompanied by a bright flash and generation of sound.

The length of the streamer discharge is controlled by shifting the tube from the microwave beam focus. The length of discharge is about 180 mm if the initiator is located at the focus. It decreases shifting the initiator. Measurements of the length of discharge and propagation speed of the combustion front is based on the post-processing of the videos taken with 10000 frames/ s (Figure 12). The first frame shows the glow from the streamer discharge. Dark vertical lines correspond to the external elements of the experimental setup.
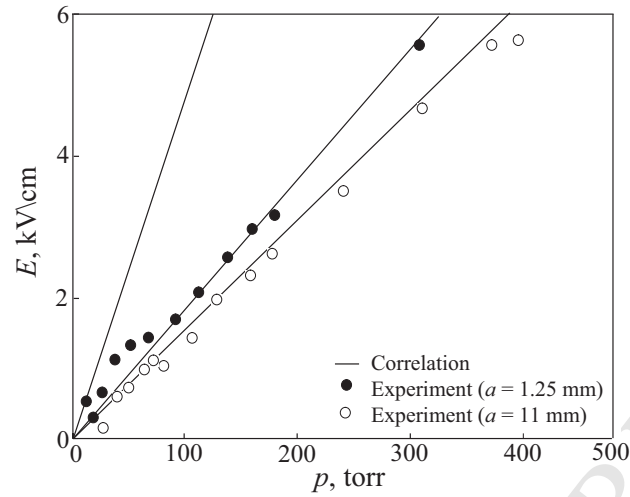
Figure 10. Comparison of threshold of air break-down (line 1) with threshold value in the presence of metallic sphere with radius $a = 1.25$ mm (line 2, •) and radius $a = 11$ mm (line 3, ∘)
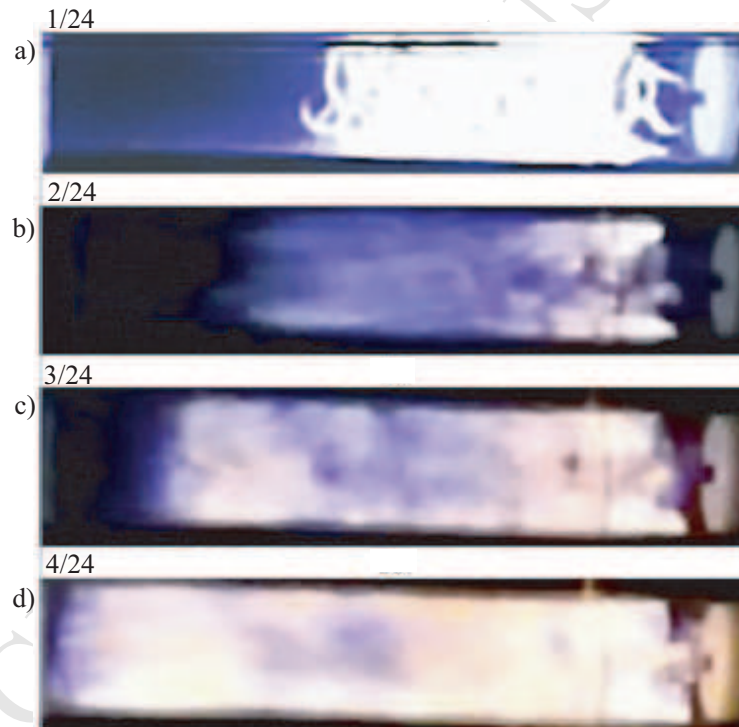

Figure 11. Development of combustion front for $E_0 = 2.4$ kV/cm and length of streamer discharge 140 mm. The camera speed is 24 frames/s

Lowering the strength of electric field to $E_0 = 1.7$ kV/cm leads to disappearing of the streamer discharge and formation of diffuse attached discharge shown in the Figure 13. The speed of combustion front is 0.15 m/s. The character of the flame propagation corresponds to the classical theory of diffusive laminar flame, mechanism of which propagation is related to the thermal effects. Diffuse regions on the ends of initiator ignite the air-fuel mixture, and two combustion waves, which are spherical at the initial time moment, propagate through the mixture. At the certain distance from end of the tube these waves begin to interact leading to the formation of plane combustion front propagating to the open (sealed) end of
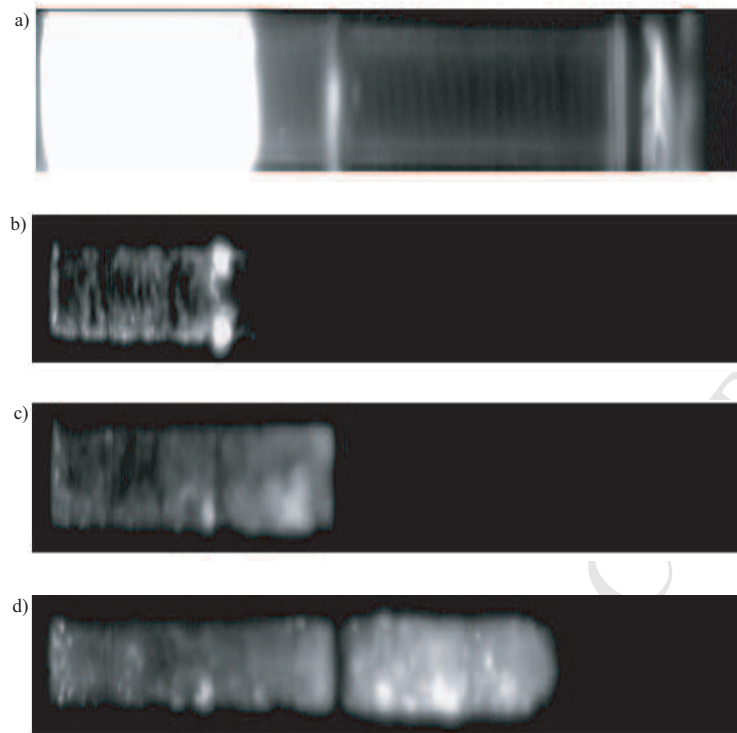
Figure 12. Development of combustion front. The camera speed is 8900 frames/s. Fragments a–d show time evolution of the mixture in a tube

the tube. Reaching the sealed end, the membrane damages, and combustion products are rejected to the atmosphere.
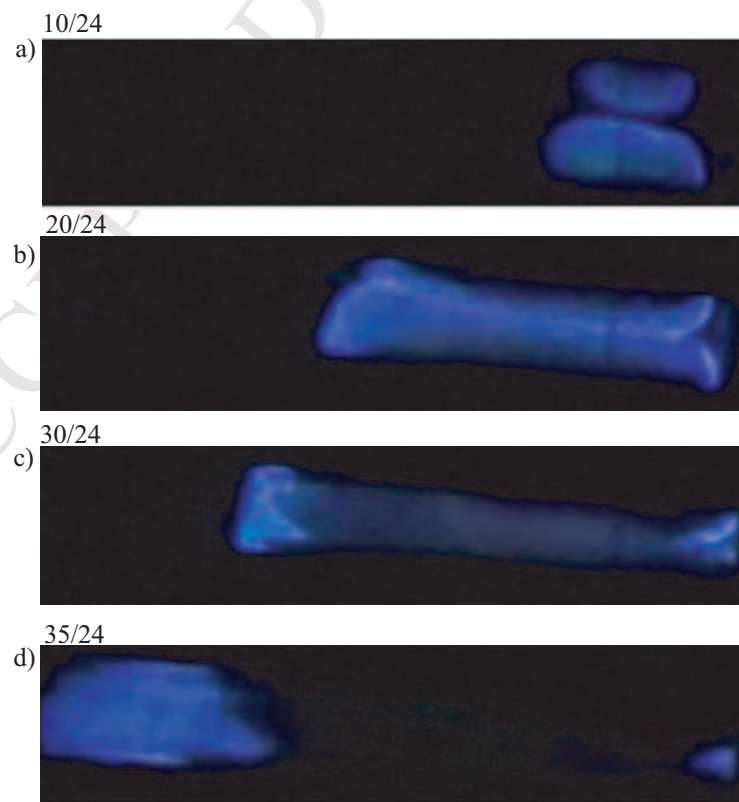

Figure 13. Development of combustion front for $E_0 = 1.7$ kV/cm. The camera speed is 24 frames/s

High-speed camera with a frame speed of 1200 frames/s allows to measure the flame propagation speed with the ignition of the mixture induced by deep subcritical streamer discharge. Spatial-temporal diagrams, typical one is presented in the Figure 14, are used in post-processing of the measured data. There are two slopes in the ignition kernel growth rate. The steeper slope persists while the discharge pulse burst is active, and represents the growth of the plasma volume as it is transported downstream by the flow. The second slope represents the ignition kernel expansion in the absence of the plasma. This is only a function of the flame speed, and is not affected by the plasma volume. In this case, the length of tube occupied by the streamer discharge is about 15 cm, and flame propagation speed is about 160 m/s. The flame front propagates with high speed while combustion waves from the discharge initiators merge on the tube centreline. Then, propagation speed decreases due to appearance of the rarefaction wave propagating towards closed end. A flame propagating from the open channel end to the closed one interacts with acoustic waves reflected form the closed end, leading to folding of the flame shape.
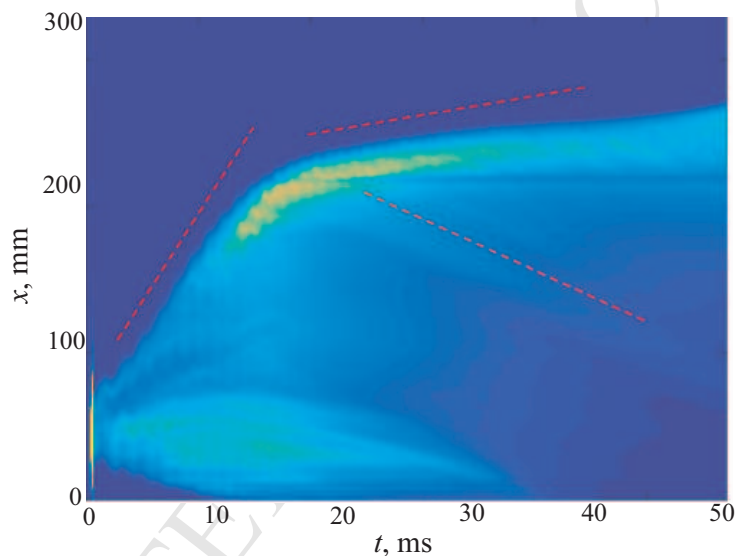

Figure 14. Typical spatial-temporal diagram used for measurement of propagation speed of the flame (dependance of coordinate of front location on time)

The velocity of the flame front has been measured with an array of photodiodes set along the tube wall and, independently, from photographic records. The experimental results on flame propagation speed are presented in the Figure 15 (symbols ○). Vertical lines show experimental uncertainties. The probability of ignition is found by attempting to ignite the mixture six times for each condition and recording how many ignition events were successful. The measurement uncertainties are calculated from the standard deviation of the test images. Dependance of the flame propagation speed on the length of streamer discharge is close to the linear.

Direct measurements of the gas temperature in the streamer are difficult. The analysis of the temperature using numerical simulations complements the investigation of streamer discharges and allows to interpret the experimental findings. The effect of ignition area on the propagation of a premixed laminar flame in axisymmetric channel has been obtained with the numerical model. Figure 15 shows comparison of experimental (symbols ○) and computational (symbols ●) results for stoichiometric mixture. The simulation results fit well the experimentally measured quantities.

The time needed to burn the whole amount of gas is dependent on the amount of elec-
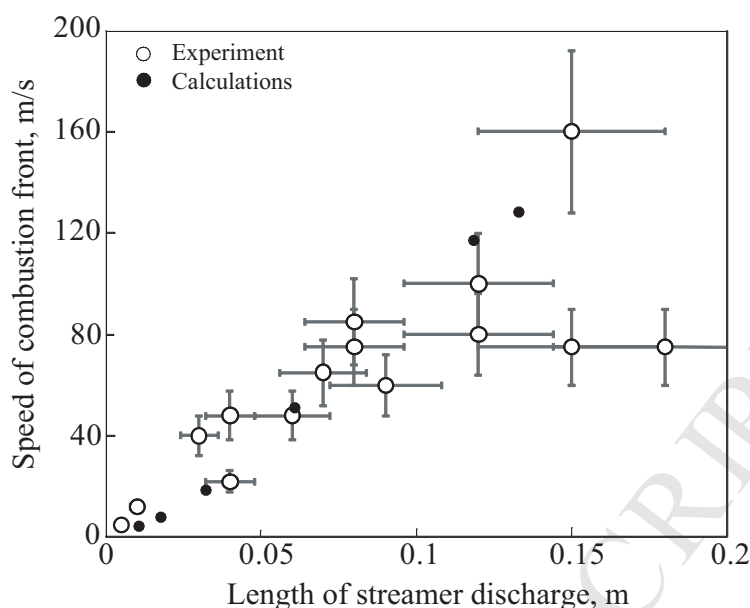
Figure 15. Dependance of the propagation speed of flame front in the quartz tube, filled by air/propane mixture, on the length of the streamer discharge, initiated on the internal surface of the tube

trical energy released into the gas. Ignition is promoted by thinner plasma channels, where the energy density is higher. The ability of the discharge to ignite air/propane mixtures, even at low equivalence ratios, is strongly correlated to the energy density that the discharge is able to release into the gas. The higher propagation speed is the result of the higher flame surface area evolved from the larger ignition areas. The flame propagation speed becomes very high due to the enlargement of flame surface area caused by the larger ignition area, and consequently, flame propagation time in the channel is reduced.

Figure 16 shows combustion patterns induced by spark ignition and deep subcritical streamer discharge at the atmospheric pressure and air-to-fuel ratio close to the lower flammability limit. The flame propagation speed is about 1 m/s in both cases (the combustion wave propagates from the right to the left). However, flame color is yellow in the case of spark ignition (Figure 16a) demonstrating incomplete combustion. Streamer discharge ignition leads to blue flame (Figure 16b) with complete combustion of the mixture. The bright points correspond to the initiator. The distance between ends of initiator is 32 mm. The strength of electric field is 1 kV/cm.
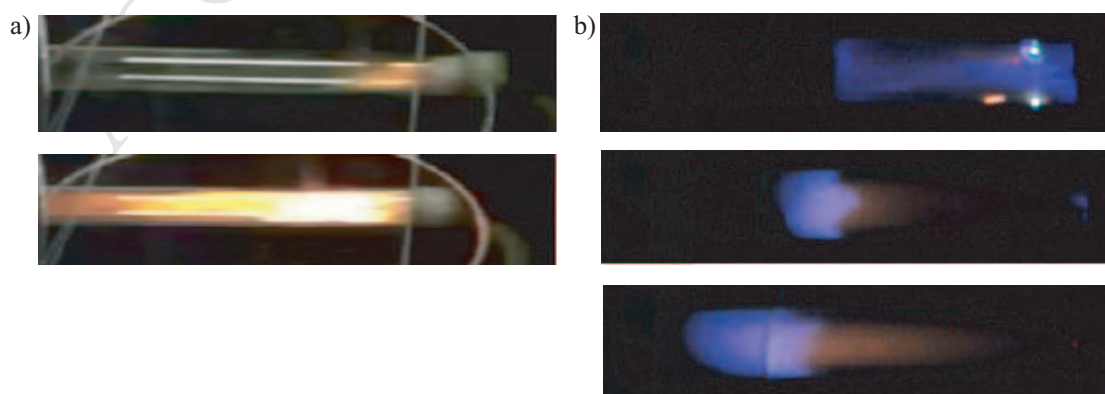

Figure 16. Comparison of spark ignition (a) and streamer discharge ignition (b). The camera speed is 24 frames/s

The propagation speed of laminar flames of hydrocarbon/air mixtures is much smaller than the sound speed in the fresh gas. The flow ahead of the flame is strongly subsonic and almost isobaric. However, even slow premixed flames may spontaneously accelerate, compress the unburned mixture and eventually trigger detonation. This phenomenon of deflagration to detonation transition (DDT) has been widely observed, particularly in experiments on flame propagation in tubes. Indeed, the prevention or safe inducement of DDT is one of the key unsolved problems in combustion research.

Streamer discharge ignition provides shorter burn duration than flames ignited by spark plugs, even at the most favorable spark location. Streamer discharge creates several hundred discharge channels filling the tube, and a significant fraction of these channels produce successful ignition kernels. The distance and time each kernel must travel to consume combustible mixture is reduced compared to spark ignition.

6   Conclusion

Ignitable area becomes one of the key parameters in addition to minimum ignition area. The streamer discharge produces multiple filaments that can initiate ignition along the plasma channels, providing a volumetric ignition process as the streamers sweep a much larger volume compared to the conventional spark ignition. The effect of ignition surface area on the propagation of a premixed flame is investigated experimentally and numerically in an axisymmetric channel.

A stable ignition of the premixed air/propane mixture with the deep subcritical streamer discharge initiated on the internal surface of quartz cylindrical tube is achieved. The microwave streamer discharge is able to ignite air/propane mixtures at a low initial temperature and atmospheric pressure. Ignition of the air/propane mixture by a subcritical streamer discharge yields more than fourfold, from 5 m/s to 150 m/s, increase in combustion speed compared to conventional spark ignition. A possibility of achievement of flame speeds larger than 100 m/s, corresponding to deflagration to detonation transition, is demonstrated. A major cause of the flame acceleration is an increase in the flame surface area and thereby the total heat release rate.

The more rapid combustion with streamer discharges could be exploited in practical combustion devices. Increase in flame surface, caused by the large ignition area, is one of the potential methods in improving combustion efficiency by reducing the burning time in the propulsion systems. The microwave streamer ignition can be considered for the application in internal combustion engines to replace the conventional spark ignition. Pulsed detonation engines are currently being evaluated for high-speed propulsion systems. Streamer discharge ignition could provide shorter deflagration to detonation lengths with fewer obstacles that generate pressure drops and heat losses.

Acknowledgements

References

[1] Phylippov Yu.G., Dushin V.R., Nikitin V.F., Nerchenko V.A., Korolkova N.V., Guendugov V.M. Fluid mechanics of pulse detonation thrusters. Acta Astronautica, 2012, 76(1), 115–126.

[2] Smirnov N.N., Betelin V.B., Nikitin V.F., Phylippov Yu.G., Jaye Koo. Detonation engine fed by acetylene-oxygen mixture. Acta Astronautica, 2014, 104(1), 134–146.

[3] Lackner M., Winter F., Graf J., Geringer B., Weinrotter M., Kopecek H., Wintner E., Klausner J., Herdin G. Laser ignition in internal combustion engines — a contribution to a sustainable environment. Proceedings of the 14th IFRF Members Conference, 11–14 May 2004, Noordwijkerhout, The Netherlands.

[4] Cathey C.D., Tang T., Shiraishi T., Urushihara T., Kuthi A., Gundersen M.A. Nanosecond plasma ignition for improved performance of an internal combustion engine. IEEE Transactions on Plasma Science, 2007, 35(6), 1664–1668.

[5] Matveev I., Matveeva S., Serbin S. Design and preliminary result of the plasma assisted tornado combustor. AIAA Paper, 2007, 2007-5628.

[6] Davydov A.M., Gritsinin S.I., Kossyi I.A., Shikhman Y.M., Vinogradov V.A. Application of MW plasma generator for ignition of kerosene/air mixture. IEEE Transactions on Plasma Science, 2008, 36(6), 2909–2917.

[7] Dresvin S., Zverev S., Ivanov D., Matveev I. High frequency induction plasma torches. Plasma Assisted Combustion, Gasification, and Pollution Control. Vol. I. Methods of Plasma Generation for PAC. Outskirts Press, 2013, 373–462.

[8] Loktionov E.Y., Pasechnikov N.A., Telekh V.D. Laser-induced breakdown ignition in a gas fed two-stroke engine. Journal of Physics: Conference Series, 2018, 946, 012066 (5 pages).

[9] Ju Y., Sun W. Plasma assisted combustion: dynamics and chemistry. Progress in Energy and Combustion Science, 2015, 48, 21–83.

[10] Sun J., Wang W., Yue Q., Ma C., Zhang J., Zhao X., Song Z. Review on microwavemetal discharges and their applications in energy and industrial processes. Applied Energy, 2016, 175, 141–157.

[11] Starikovskiy A., Rakitin A. Plasma-assisted ignition and deflagration-to-detonation transition. AIAA Paper, 2015, 2015-1601 (18 pages).

[12] Lefkowitz J.K., Ombrello T. Study of nanosecond pulsed high frequency discharge ignition in a flowing methane/air mixture. AIAA Paper, 2017, 2017-1777 (10 pages).

[13] Uddi M., Guo H., Sun W., Ju Y. Studies of C_2H_6/air and C_3H_8/air plasma assisted combustion kinetics in a nanosecond discharge. AIAA Paper, 2011, 2011-970 (14 pages).

[14] Carbone E., Sadeghi N., Vos E., Hűubner S., van Veldhuizen E., van Dijk J., Nijdam S., Kroesen G. Spatio-temporal dynamics of a pulsed microwave argon plasma: ignition and afterglow. Plasma Sources Science and Technology, 2015, 24(1), 015015 (17 pages).

[15] Shishpanov A.I., Meshchanov A.V., Kalinin S.A., Ionikh Y.Z. Processes of discharge ignition in long tubes at low gas pressure. Plasma Sources Science and Technology, 2017, 26(6), 065017 (12 pages).

[16] Fuh C.A., Wu W., Wang C. Microwave plasma-assisted ignition and flameholding in premixed ethylene/air mixtures. Journal of Physics D: Applied Physics, 2016, 49(28), 285202 (14 pages).

[17] Esakov I., Grachev L., Khodataev K., Van Wie D. The linear electromagnetic vibrator as the initiator of electric breakdown of air in deeply subcritical field of quasioptical microwave beam. AIAA Paper, 2011, 2011-1151 (12 pages).

[18] Khodataev K.V. Numerical modeling of the combustion, assisted by the microwave undercritical discharge in supersonic flow. AIAA Paper, 2005, 2005-0985 (6 pages).

[19] Dhali S.K., Williams P.F. Two-dimensional studies of streamers in gases. Journal of Applied Physics, 1987, 62(12), 4696–4707.

[20] Naidis G.V. On photoionization produced by discharges in air. Plasma Sources Science and Technology, 2006, 15(2), 253–255.

[21] Kulikovsky A.A. The role of photo-ionization in positive streamer dynamics. Journal of Physics D: Applied Physics, 2000, 33(12), 1514–1524.

[22] Pancheshnyi S.V., Starikovskaia S.M., Starikovskii A.Y. Role of photoionization processes in propagation of cathode-directed streamer. Journal of Physics D: Applied Physics, 2001, 34(1), 105–115.

[23] Khodataev K.V. The nature of surface MW discharges. AIAA Paper, 2010, 2010-1378 (10 pages).

[24] Georghiou G.E., Morrow R., Metaxas A.C. A two-dimensional finite element-flux corrected transport algorithm for the solution of gas discharge problems. Journal of Physics D: Applied Physics, 2000, 33, 2453–2456.

[25] Aleksandrov K.V., Grachev L.P., Esakov I.I., Fedorov V.V., Khodataev K.V. Domains of existence of various types of microwave discharge in quasi-optical electromagnetic beams. Technical Physics, 2006, 51(11), 1448–1456.

[26] Grachev L.P., Esakov I.I., Mishin G.I., Khodataev K.V. Front velocity of stimulated discharge in microwave beam. Technical Physics, 1995, 65(5), 21–30.

[27] Takahashi M., Ohnishi N. Shock formation by plasma filaments of microwave discharge under atmospheric pressure. Journal of Physics: Conference Series, 2016, 688, 012119 (4 pages).

[28] Volkov K. Multigrid and preconditioning techniques in CFD applications / CFD Techniques and Thermo-Mechanics Applications. Springer International Publishing, 2018, 83–149.

Ignition and Combustion of Air/Fuel Mixture in a Long Tube Induced by Microwave Subcritical Streamer Discharge

M.P. Bulat[1], P.V. Bulat[1, 2], P.V. Denissenko[3], I.I. Esakov[4], L.P. Grachev[4], K.N. Volkov[5], I.A. Volobuev[1]

[1]Baltic State Technical University, St Petersburg, Russia
[2]ITMO University, St Petersburg, Russia
[3]University of Warwick, Coventry, United Kingdom
[4]Moscow Radiotechnical Institute of Russian Academy of Sciences, Moscow, Russia
[5]Kingston University, London, United Kingdom

- Amplitude of initial electric field is lower than the critical one
- Possibility of ignition and combustion with streamer discharge is studied
- Streamer discharge ignition of a stoichiometric fuel mixture is demonstrated
- Streamer discharge yields improvement of combustion speed and efficiency